# The M.A.C.'07 MAV

M. Müller, A. Schröter, C. Lindenberg
Team M.A.C., Hildesheim, Germany

**Abstract:**

The M.A.C.'07 MAV project deploys an autonomous, delta shaped, electrically propelled fixed wing airplane made from expanded polypropylene (EPP) for the outdoor task and a coaxial helicopter with 35cm rotor diameter for the indoor task.
The outdoor MAV propulsion system consists of an electronically commuted, brushless electric motor and lithium polymer cells. Six infrared thermopiles are used for attitude detection, a GPS receiver for 3D position and direction determination, and a color CCD camera for observation. Video is transferred live through a 2.4GHz downlink. Telemetry data is exchanged through a bidirectional 868MHz link. Its autonomous flight control system is based on a 32 bit micro controller. The controller compares the current GPS position and direction with waypoints of a predefined mission to calculate desired intermediate positions, target values for turn, climb and roll rates and the corresponding settings of the tailerons. It also controls a one axis stabilized tilt camera as well as a paint ball release mechanism. A safety 41MHz uplink remote control signal can be used to switch between manual and autonomous control. The flight control hard- and software are derived from the Paparazzi project [1].

The indoor MAV is based on the mechanics of a commercially made RC helicopter. It is manually controlled using real time video for navigation outside the line of sight of the pilot. The yaw movement is gyro stabilized. The camera's tilt angle can be changed in flight.
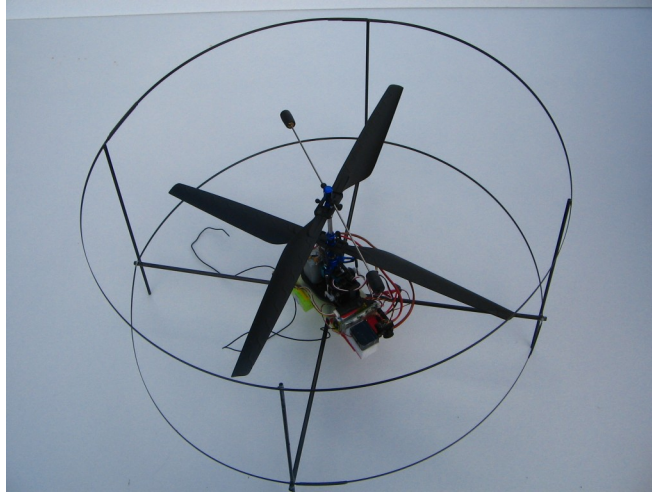


*Fig. 1: Indoor MAV with anti collision cage*

**Motivation**

The outdoor MAV is the evolutionary advancement of our preceding competition aircrafts from 2005 and 2006. All operations of the outdoor aircraft are fully autonomous, including the paint ball deployment.

**Indoor MAV**

Due to its inherent in-flight stability and the lack of a protruding tail boom a helicopter with coaxial rotors is used for the indoor MAV (cp. Fig. 1). Each of the two rotors has its own, separately controlled electric motor. Lift is increased/decreased by simultaneously increasing/decreasing the the rotary speeds of both motors. Yaw can be controlled via the rotary speed difference of both motors. There is no collective pitch control. The lower rotor is equipped with a swash plate for control of cyclic blade movement for pitch and roll. The top rotor is connected to a stabilizing bar. The yaw is stabilized by a micro-controller which sets the motors' speed difference in accordance to the output of an integrated piezo-ceramic gyro sensor. The rotating parts are protected by a surrounding carbon frame. The helicopter's payload consists of a colour CMOS camera and a 2.4GHz video transmitter (cp. Fig. 2). The tilt angle of the camera can be controlled through a servo. The pilot flies the aircraft observing the video transmission on a TFT screen.
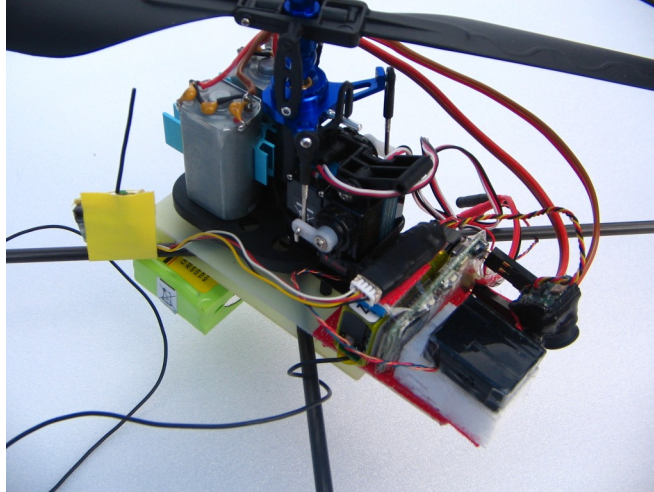
*Fig. 2: Helicopter mechanics and electronics*

**Outdoor MAV Airframe**

For the construction of the M.A.C.'07 airframe we relied on our experiences in model airplane construction and flying, especially in electric flight and construction of light foam based airframes. The aircraft is constructed from expanded polypropylene (EPP) using glass and carbon fiber reinforced tailerons. The airframe was designed using CAD software. Wings and fuselage were cut from an EPP block using a CNC hot wire cutter. Fig. 3 and 4 show the raw fuselage and the wing negatives. For the profile a well proven delta wing model airplane profile was slightly thinned to achieve higher velocities. For a satisfactory stall behavior micro turbulences generated by the rough wing skin are exploited. The EPP surface was hardened to improve its ruggedness.



*Fig. 3: Raw fuselage cut from EPP*

*Fig. 4: Wing negatives after hot wire CNC cutting*

**Sensors**

Six PerkinElmer TPS 334 infrared thermopiles are used for attitude detection (cp Fig. 5). The thermopile sensors measure far infrared radiation in the 5-14μm range. Due to the temperature difference between sky and earth the horizon can be detected by a pair of back-to-back mounted thermopiles. Two pairs of sensors are used to determine the pitch and roll angles of the airplane. The third pair is used to constantly measure the maximum infrared radiation difference between nadir and zenith for in flight calibration of the other sensors. This method works nicely on sunny and cloudy days and even in light rain. The horizon detection has its limitations on very cold days and in foggy conditions – similar to flight under visual flight rules (VFR). A detailed description can be found in Taylor et al [2]. The thermopile sensors are integrated into the aircraft's fuselage for reduced drag and vibration sensitivity as well as improved mechanical protection.
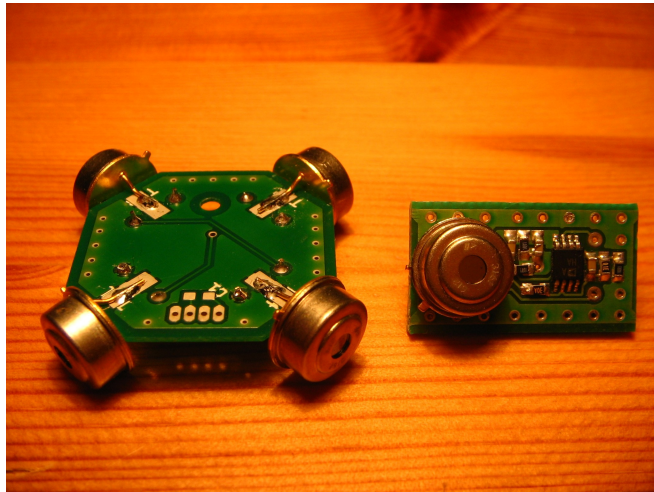

*Fig. 5: Infrared sensors for attitude detection*

An u-blox LEA-4P GPS receiver yields the 3D position and direction information. The signal is received through a circularly polarized ceramic patch antenna. Receiver and antenna are both located on the processor board and are mounted inside the aircraft.

**On board flight control**

We designed the autopilot electronics together with members of the Paparazzi project. An ARM7TDMI 32bit 60MHz processor made by Philips is used for on board flight and camera control (cp. Fig. 6). A standard 41MHz RC receiver is used as a security uplink. The autonomous operation of the processor can be overridden by manual control at any time. There is a fly-by-wire process used for evaluating the RC receiver signal and to determine auto or manual operation. In manual mode the standard RC servo signals are passed through to the servos. In auto mode the signals are generated on board by the autopilot process. It uses the attitude information from the IR sensors to set the taileron positions through PI control loops. The desired turn rate is calculated from the GPS position information and the given waypoints. The main control loop operates at 60Hz while the GPS data is updated at 4Hz. The processor load is less than 5% for the flight stabilization and waypoint calculation. The proportional and integrative values of the PI regulators were manually tuned in various test flights. The processor, GPS receiver, antenna and a switching power supply were integrated into one single board to optimize weight, size, electromagnetic interference and mechanical stability.
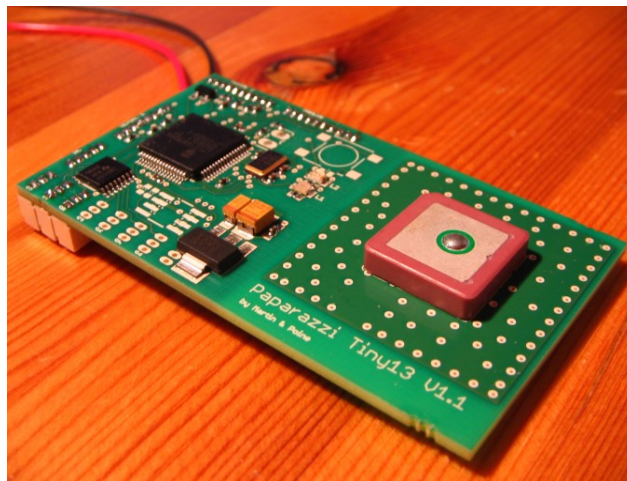

*Fig. 6: Processor board with GPS and power supply*

**Video and telemetry**

For video downlink a 2.4GHz transmitter is used. The video pictures are transmitted as an analog frequency modulated NTSC signal. A digital 868MHz transceiver is used to establish a bidirectional telemetry link (cp. Fig. 7). A number of data messages can be chosen, e.g. attitude, position, waypoints, mission status, voltages or debug information. Commands can be given during flight, e.g. change of waypoint positions or flight plan.
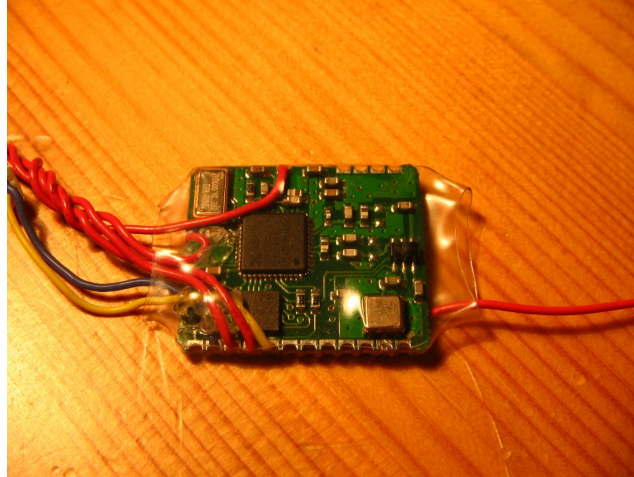
*Fig. 7:  868MHz telemetry transceiver, antenna*

**Ground control station**

The ground control station (GCS) consists of an analog 2.4GHz video receiver, a TFT monitor, a laptop computer and a 868MHz modem that is connected through USB. Additionally a video encoder can be used. The video is shown on a separate TFT screen.

The telemetry data is decoded in the laptop computer and various aircraft parameters can be displayed. The aircraft position is shown using Google Maps (cp. Fig. 8).

Flight plans are generated using a script language. Waypoints can be set and changed through the graphical interface of the GCS system. The flight plan is downloaded to the aircraft using USB. In flight the  flight plan flow and waypoints as well as control parameters can be adjusted.
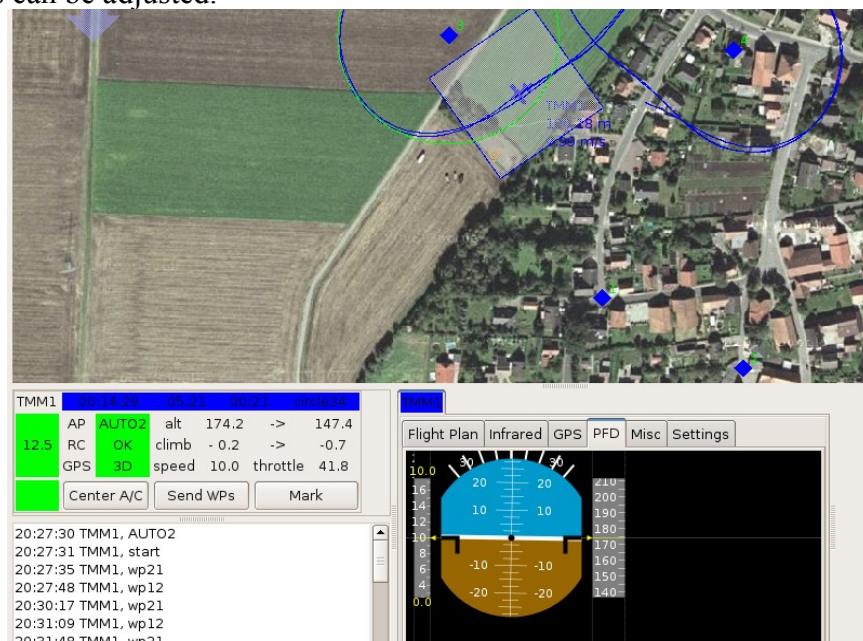


*Fig. 8: Paparazzi ground control station software utilizing Google Maps*

**Stabilized camera**

The camera mounting consists of a servo for tilt movements carrying a fixed focus CCD camera (cp. Fig. 9). Using the position, direction and attitude information from the flight control system the tilt angle is calculated in such a way that the camera observes an object under the planes flight path regardless of the planes movement. To search an area this object position can be shifted in flight via the 868MHz telemetry link.



*Fig. 9: CCD Camera in the MAV's nose*

To keep the overall weight as low as possible the camera tilt mechanics in the MAV's nose is used for the paint ball release as well (cp. Fig. 10).



*Fig. 10: Camera mounting and paint ball deployment payload bay*

**Paint ball deployment**

To determine a well suited release position for the paint ball the following approach is used:

The trajectory of the ball is influenced by the MAV's position, flight direction, angle of climb and speed in the moment of release as well as by air drag and wind during the ball's fall.

The paint ball's equation of motion may be written as:

$$m \ddot{\vec{r}} = \vec{F} = -\alpha (\dot{\vec{r}} + \vec{v_{Wind}}(z))^2 \frac{\dot{\vec{r}} + \vec{v_{Wind}}(z)}{|\dot{\vec{r}} + \vec{v_{Wind}}(z)|} - mg\,\vec{e}_z$$

With

| | | |
|---|---|---|
| $m$ : | mass of the ball (3.31g) | |
| $\ddot{\vec{r}}$ : | acceleration of the ball | |
| $\vec{F}$ : | sum of all external forces | |

$$\alpha = \frac{1}{2} \rho A c_w$$

| | |
|---|---|
| $A = \pi R^2$ : | cross section area of the ball |
| $R$ : | radius of the ball (17.3mm) |
| $c_w$ : | drag coefficient of a sphere (0.45) |
| $\rho$ : | density of air depending on pressure, temperature and humidity (1.184 kg/m³ at standard conditions) |
| $\vec{r}$ : | position of the ball |
| $v_{Wind}(z)$ : | wind velocity vector depending on the altitude (wind shear) |
| $\dot{\vec{r}}$ : | velocity of the ball |
| $g$ : | gravitational acceleration (9.81 kg m/s²) |
| $\vec{e}_z$ : | unit vector in vertical direction |

This set of three coupled non linear differential equations is solved numerically using the Euler method:

$$\partial \vec{r} = \dot{\vec{r}} \, \partial t$$
$$\partial \dot{\vec{r}} = \frac{\vec{F}}{m} \partial t$$

The initial conditions for the computation are

$$\vec{r}(t=0) = \text{position of the MAV in the moment of release}$$
$$\dot{\vec{r}}(t=0) = \text{velocity of the MAV in the moment of release}$$

Fig. 11 shows calculated trajectories for a paint ball, which is released from an MAV

flying with 25m/s speed in 30m altitude at different wind speeds. For comparison the trajectory for a ball without any air drag (parabola) is included.

The curves show quantitatively what one expects intuitively: the stronger the head wind, the shorter the deployment distance (horizontal distance between release position and deployment position).
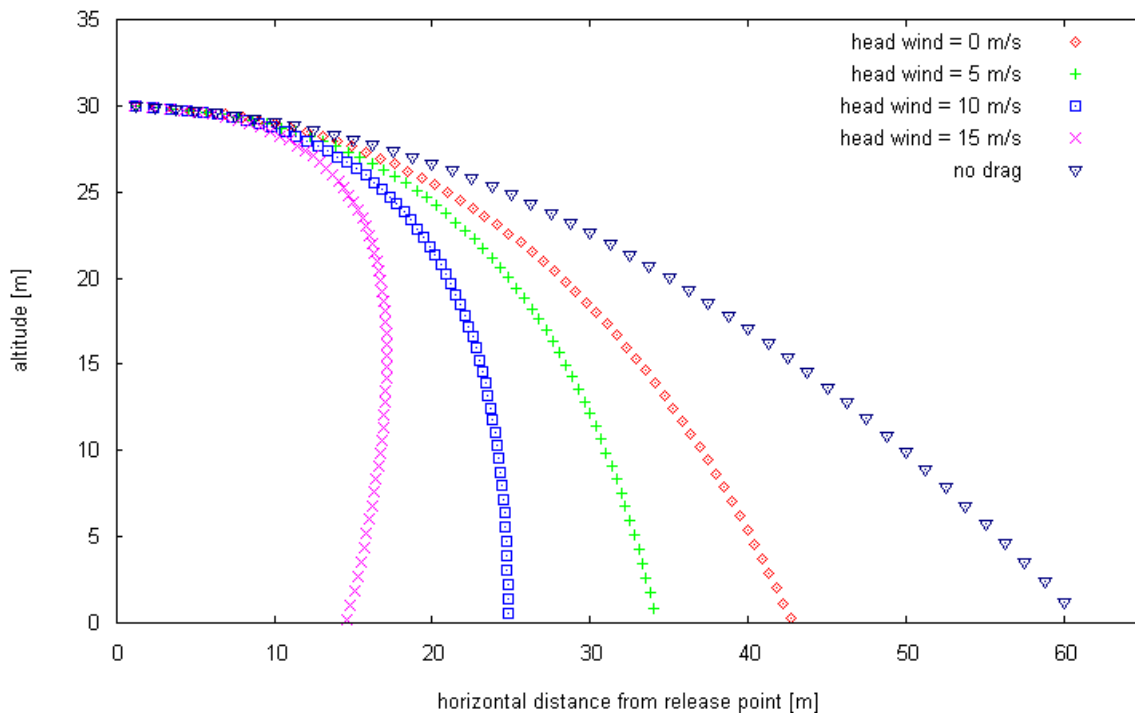


*Fig. 11: Paint ball trajectories for different wind speeds (initial velocity 25m/s, release altitude 30m). For comparison the trajectory for a ball without any air drag (parabola) is shown*

To verify the numerical algorithm its results for some situations were compared with their analytical solutions:

- release of an object with no air drag, which results in a parabola shaped trajectory (cp. rightmost curve in Fig. 11)
- release of an object at very large altitudes reaching its terminal velocity

Furthermore reverse trajectories were calculated using time reversal to compare the final result with the initial conditions.

With 50ms time steps the numerical impact position error using the Euler method is less than 10cm. A Runge-Kutta approach might be used to optimize computing effort.

In flight the onboard computer calculates the ball trajectory 20 times per second using the current flight parameters (altitude, speed, direction, climb angle) and the wind direction and speed transmitted by the ground station. The difference between the calculated impact point and the desired deployment position is used to determine a suitable release position for the MAV.

As soon as the MAV reaches this position the ball is released automatically.

Flight tests showed a typical deployment accuracy of 16m at wind speeds of 4-7 m/s (release altitude 60m, MAV speed 8-10m/s).
Approaches can take place in any direction relative to the wind direction.

Three methods were considered for paint ball deployment: release from horizontal flight, from a dive and from a climb.

The maximum deployment distance is reached at 18º climb angle.

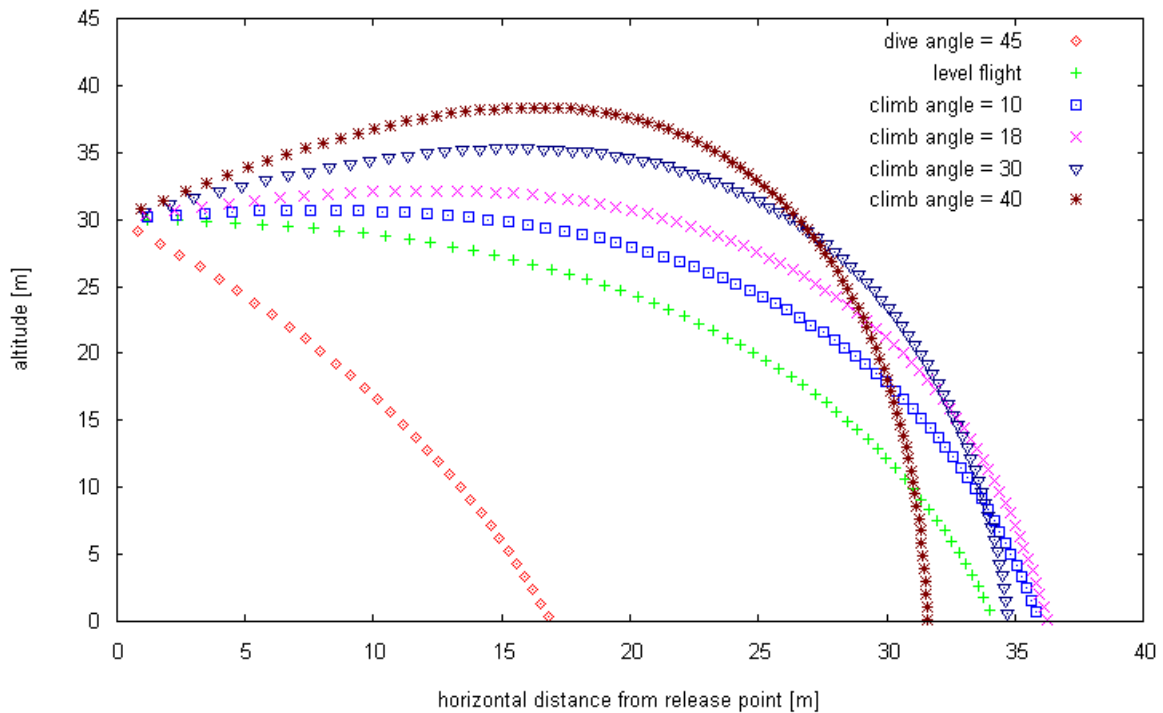Fig 12. shows the ball trajectories for releases at various climb/dive angles.



*Fig. 12: Paint ball trajectories for MAV speed 25m/s, wind speed 5m/s and various climb angles*

For a quantitative comparison of the deployment methods the deployment distances as well as the influence of flight parameter error on the deployment accuracy were calculated (Tab. 1):

| | 45° dive | horizontal flight | 18° climb |
|---|---|---|---|
| deployment distance | 17,1 m | 34,2 m | 36,3m |
| wind speed | 0,7 m / (m/s) | 1.7 m / (m/s) | 2,5 m / (m/s) |
| wind direction (head wind 10 m/s) | 0.0005 m / ° in flight direction 0.046 m / ° perpendicular to flight direction | 0.0013 m / ° in flight direction 0.1 m / ° perpendicular to flight direction | 0.0018 m / ° in flight direction 0.15 m / ° perpendicular to flight direction |
| release height | 0,26 m / m | 0,4 m / m | 0,11 m / m |
| release velocity | 0,27 m / (m/s) | 1,3 m / (m/s) | 1,13 m / (m/s) |
| plane direction | 0,49 m / ° | 0,7 m / ° | 0,83 m / ° |
| plane climb angle | 0,34 m / ° | 0,3 m / ° | 0,0 m / ° |
| release time | 10,2 m / s | 25 m / s | 24,5 m / s |
| release position in / perpendicular to flight direction | 1 m / m (simple offset) | 1 m / m (simple offset) | 1 m / m (simple offset) |
| paint ball weight | 1,2 m / g | 4,8 m / g | 6,2 m / g |
| paint ball diameter | 0,65 m / mm | 2,1 m / mm | 2,7 m / mm |
| barometric pressure | 0,008 m / mbar | 0,02 m / mbar | 0,024 m / mbar |

*Tab. 1: Deployment distances and deployment errors for release from dive, level flight and climb. The error values give the deviation from the optimum deployment position depending on inaccuracies of the corresponding flight parameters, environmental conditions and ball properties (partial derivatives)*

The initial conditions for the calculations were
      MAV speed at the release point:    25 m/s
      MAV angle of climb:    -45° dive, 0° level flight, 18° climb
      Release altitude:    30 m
      Head Wind:    5 m/s
In each line the most desirable values are marked in yellow.

Due to the paint ball's high drag to weight ratio release from a climb yields an only slightly larger deployment distance compared to release from level flight.

The best error tolerance for almost all flight parameters can be achieved using dive release, because this deployment mode results in the shortest paint ball flight distance and flight time.
The disadvantages of a dive release in comparison to the other release modes are:
- the MAV gets closer to the ground which reduces safety and increases the noise level at the deployment site and thereby the probability of detection.
- controlling a steep dive close to the ground increases the requirements on the flight control system considerably.

Trading precision for safety we will release the paint ball from level flight.

**Security provisions**

The two process concept minimizes risks due to faulty software. The fly-by-wire process evaluates the incoming RC signals and generates the servo PPM signals only. Its code is small, simple, very well tested and rarely modified. The larger and more complex software for sensor data evaluation, flight and camera control is running in the separate autopilot process. In this way it is always possible to return to manual control even if unforeseen software problems occur in the autopilot process.

Prior to each flight a software-in-the-loop-test can be executed in the ground station software environment to simulate the mission and to detect errors without putting people, property or the airplane at risk. Whenever a loss of the uplink RC connection or telemetry link is detected or when predefined no fly zones are entered the plane automatically aborts its mission and tries to return to a predefined home position. Alternatively the flight control system can be programmed to shut down the motor and put the airplane into a shallow dive in such a situation.

Additional details on safety measures can be found in the separate security memo.

**Test flight data**

The flight parameters recorded during a test flight are shown in Fig. 13-18. The aircraft covers a distance of approx. 150m three times from west to east and back again (cp. Fig. 13). The flight control system is configured to keep the aircrafts altitude constant using throttle and elevator. Passes from west to east are a little bit faster than vice versa, since the wind was coming from south west (cp. duration of upwind and downwind legs in Fig. 13 and speed in upwind and downwind legs in Fig. 17). The MAV's average ground speed is ~12m/s in upwind legs and turns and ~16m/s in downwind legs while it accelerates to 24m/s in downwind turns (cp. Fig 17). Bank angles during turns are approx. 15° (cp. Fig. 15). At the downwind turn point turns take approx. 10s, while the upwind turns are considerably shorter (cp. Fig 15).
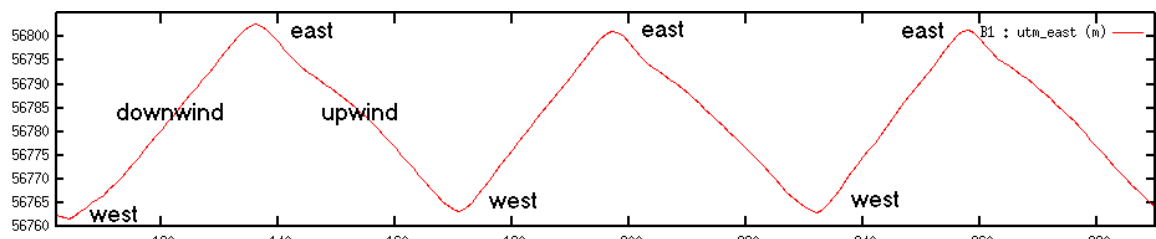
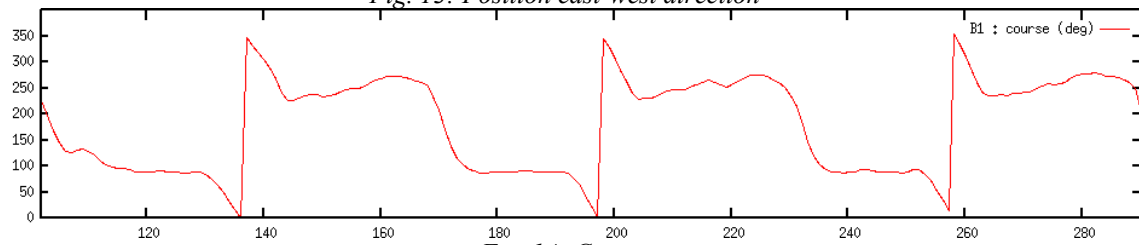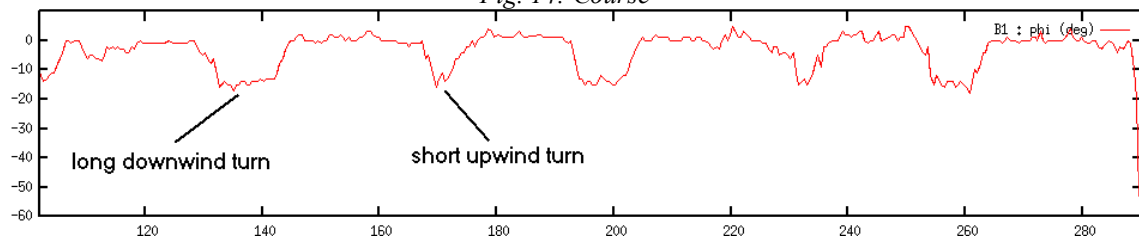*Fig. 13: Position east-west direction*
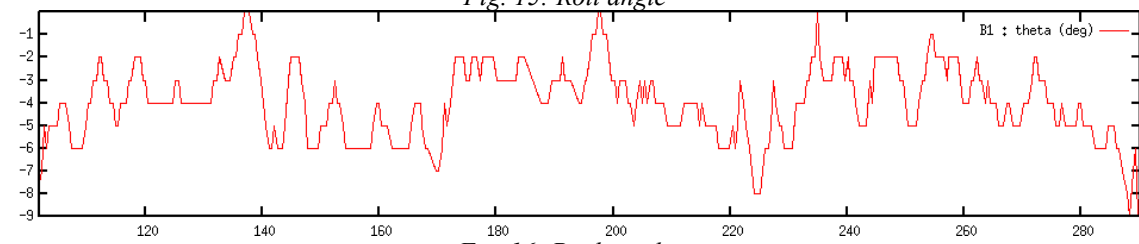

*Fig. 14: Course*
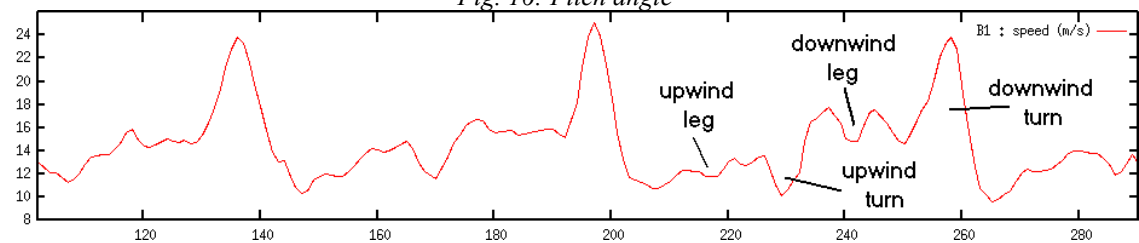

*Fig. 15: Roll angle*


*Fig. 16: Pitch angle*
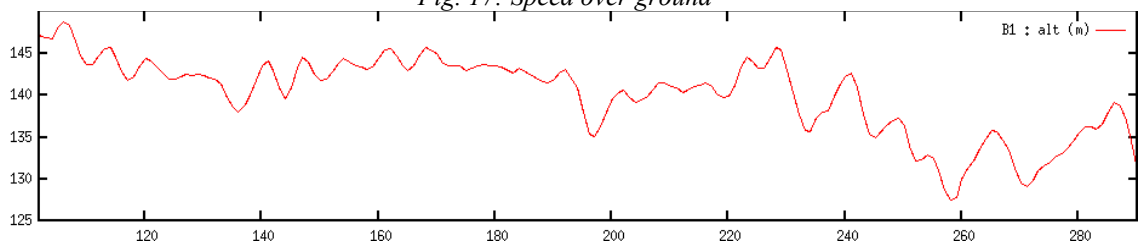

*Fig. 17: Speed over ground*


*Fig. 18: Altitude*

Team M.A.C.

**Weights and dimensions**

The aircrafts wingspan is 46cm and its length is 37cm. Considerable effort went into the weight reduction of the electronics components. The autopilot processor, the GPS receiver, its antenna and the power supply were integrated into one single board to minimize weight.

| *module* | *weight* |
| --- | --- |
| airframe | 55g |
| engine w/ controller | 30g |
| propeller | 2g |
| battery | 62g |
| infrared sensors | 14g |
| processor board, GPS receiver, antenna, power supply | 25g |
| flight servos | 10g |
| 868MHz telemetry transceiver | 6g |
| 41MHz receiver | 8g |
| 2,4GHz video transmitter | 8g |
| paint ball release mechanism, camera unit w/ tilt servo | 25g |
| total | 245g |

**Acknowledgements**

This project relies heavily on the Paparazzi project [1]. It would have been impossible to achieve autonomous flight without the generous open source idea and the fabulous work of Pascal Brisset, Antoine Drouin and many others.

**References**

[1] P. Brisset, A. Drouin: "Paparazzi project, http://www.nongnu.org/paparazzi"
[2] B. Taylor, C. Bil, S. Watkins, G. Egan: "Horizon Sensing Attitude Stabilization: A VMC Autopilot"